Journal of Organometallic Chemistry, 437 (1992) 323–346
Elsevier Sequoia S.A., Lausanne
JOM 22745

Synthesis, structure and redox chemistry of ferrocenylsilylmethylidinetricobaltnonacarbonyl complexes, $FcSi(R)_2CCo_3(CO)_9$, 1,1′-Fc′$[Si(R)_2CCo_3(CO)_9]_2$ (R = Me, Et, Ph) and their derivatives *

Jan Borgdorff, Evert J. Ditzel, Noel W. Duffy, Brian H. Robinson and Jim Simpson

Department of Chemistry, University of Otago, P.O. Box 56, Dunedin (New Zealand)

(Received February 27, 1992)

Abstract

Reaction between the ferrocenyl silanes $FcSiR_2H$ and 1,1′-Fc′$[SiR_2H]_2$ (R = Me, Et, Ph) and $HCCo_3(CO)_9$ gives the corresponding ferrocenylsilylmethylidinetricobaltnonacarbonyl complexes $FcSi(R)_2CCo_3(CO)_9$ and 1,1′-Fc′$[Si(R)_2CCo_3(CO)_9]_2$ in good yield. Spectroscopic data include ^{29}Si NMR. The crystal structure of 1,1′-Fc′$[Si(Me)_2CCo_3(CO)_9]_2$ has been determined by an X-ray diffraction study. Thermal and electron-transfer catalysed substitution reactions with Lewis bases were successful except for the cluster 1,1′-Fc′$[Si(Ph)_2CCo_3(CO)_9]_2$, where an unusual cleavage of the Fc–Si bond takes place. Electrochemical and ESR studies of the complexes $FcSi(R)_2CCo_3(CO)_9$ and 1,1′-Fc′$[Si(R)_2CCo_3(CO)_9]_2$ (R = Me, Ph) showed a one-electron oxidation centred on the ferrocenyl moiety and a one- or two-electron reduction dependent on the number of CCo_3 redox centres. The observed electrochemistry is consistent with electrochemically non-interacting redox centres. Chemical oxidation of $FcSi(Me)_2CCo_3(CO)_9$, 1,1′-Fc′$[Si(Me)_2CCo_3(CO)_9]_2$ and $FcSi(Me)_2CCo_3(CO)_8L$ (L = $P(OMe)_3$, PPh_3, PCy_3) gave the respective monocations, whereas oxidation of $FcSi(Me)_2CCo_3(CO)_7[P(OMe)_3]_2$ produced a dication.

Introduction

The view that organometallic substrates could be useful precursors for molecular devices and conducting materials [1] has been highlighted recently by, first, Aviram's suggestion [2] that fused conducting polymers did not necessarily need to have a π-framework and, second, the realisation that chemical vapour deposition (CVD) techniques do not require high vapour pressures for the substrates [3]. Organometallic clusters with non-metal functionality could be possible precursors since clusters based on the tricobaltcarbon [4,5] and tricobaltbis(carbyne) [6] units with multiple redox sites participate in cooperative intramolecular interactions.

Correspondence to: Dr. B.H. Robinson or Dr. J. Simpson.

* Throughout this paper, Fc = $(\eta^5\text{-}C_5H_5)Fe(\eta^5\text{-}C_5H_4)$ and 1,1′-Fc′ = $(\eta^5\text{-}C_5H_4)Fe(\eta^5\text{-}C_5H_4)$.

Cooperative interactions in Co_3-based clusters are crucially dependent on the nature of the carbyne ligands and the relationship of the orbitals of the carbyne carbon atom to those of its substituents [4,7]. In some complexes weak interactions derived from the existence of a suitable electron conducting bridge linking the disparate redox centres through the capping carbon atom(s) result in intervalence charge transfer transitions in the near-infrared spectra [5,8], while in others these interactions are manifested in the spectroscopic and structural data [4,9,10]. Extension of this work to silicon-containing clusters was of interest given the importance of this element in modern technology. Simple μ_3-silicon capped clusters are rare, although many compounds with silicon (and germanium) bridging metal–metal bonds have been characterised [11]. Initially our strategy was to study Co_3C–Si links to see if they are wholly σ in character, or whether the filled π-orbital on the cluster does interact with an appropriate empty silicon orbital. These complexes would also allow an investigation of electron transfer processes at electrode surfaces; Co_3C–$SiCl_2(R)$ clusters are readily synthesised [12] and chemical attachment to an electrode surface via Co_3C–Si–O bonds has been achieved in these laboratories [13].

In this report we describe the synthesis, characterisation and electrochemical properties of the multiple redox centre clusters $FcSi(R)_2CCo_3(CO)_9$, 1,1′-$Fc'[Si(R)_2CCo_3(CO)_9]_2$ (R = alkyl, aryl) and Lewis base derivatives, where one or two tricobaltcarbon cluster centres are linked to a ferrocenyl moiety by μ_2-SiR_2 bridges. The volatility of these clusters also suggests that they may be useful precursors for the production of cobalt–silicon phases by CVD techniques.

Experimental section

Synthetic procedures

All reactions were carried out under dry argon in oven-dried glassware. Chloromercuriferrocene was prepared via metallation of ferrocene [14]. Lithioferrocene was prepared by lithiation of chloromercuriferrocene as described by Seyferth *et al.* [15]. In a typical experiment, carbonylation of the lithiation derivative gave the ferrocene carboxylic acid in 53% yield. 1,1′-Dilithioferrocene was prepared as the TMEDA complex [16] from ferrocene and n-butyllithium in the presence of TMEDA. The resulting complex was normally used *in situ*, but collection of the orange solid, 1,1′-$Fc'Li_2 \cdot$ TMEDA showed the yield to be *ca.* 98%. Magnesium turnings and iodine (both M & B); isopropyl bromide and TMEDA (both BDH); ferrocene (Aldrich, Merck or Strem); $HSiCl_3$, Me_2SiCl_2 (all ROC/RIC) and Me_2SiHCl, MeEtSiHCl, Et_2SiHCl, MePhSiHCl and Ph_2SiHCl (all Petrarch Systems, Inc.) were used without further purification. $(^iPr)_2SiHCl$ was prepared from the reaction of ^iPrMgBr and $HSiCl_3$ in Et_2O [17]. n-Butyllithium (Aldrich or Merck) was standardised before use by Gilman and Cartledge's method [18]. Sodium benzophenone ketyl (BPK) in THF solution was made as described previously [19].

Reactions involving ferrocene derivatives were monitored by analytical thin layer chromatography on aluminium backed silica gel, and the product mixtures were generally separated by preparative TLC or column chromatography (both on silica gel). The stability of these compounds in organic solvents was not high, and the analyses obtained generally indicate the difficulties of isolating pure com-

pounds. Infrared spectra were recorded on Perkin–Elmer 225 or Nicolet MX-S spectrometers, ^{1}H NMR on Varian EM-390 or VXR-300 spectrometers, with ^{29}Si spectra measured using the DEPT technique [20] on a Varian VXR-300 spectrometer, using TMS as an internal reference. ESR spectra were obtained on a Varian E3 spectrometer; the procedure for *in situ* electrochemical generation of radical anions has been reported previously [21]. Electron impact mass spectra were recorded on a Varian CH-7 and FAB spectra on a VG ZAB 2HF instrument at the University of Adelaide. Molecular ion *m/e* values quoted below are based on the ^{28}Si isotope. Elemental analyses were performed by the Microanalytical Service, University of Otago.

Electrochemical procedures were as described earlier [22]. The reference electrode was a solid Ag/AgCl electrode immersed directly in the solution and was calibrated *in situ* with the known electrochemically and chemically reversible couple [ferrocene]$^{+/0}$, taken as $E_{1/2} = 0.68$ V in CH_2Cl_2 [23]. Scan rates were 20 mV s^{-1} for polarographic and 50 mV s^{-1}–5 V s^{-1} for voltammetric measurements. Solutions were *ca.* 10^{-3} M in electroactive material and 0.10 M (TBAP) in supporting electrolyte.

Ferrocenylsilanes were prepared by modification of literature methods [24,25]. As the details for some derivatives are sketchy, and others are new compounds, preparations of the new silanes FcSi(^{i}Pr)$_2$H and 1,1′-Fc′[SiMe$_2$H]$_2$ are detailed below as typical procedures (further details are available from the authors). The mono- and bis(silyl) compounds are orange/red oils, unaffected by air or water. In chlorinated solvents, especially in the presence of light, oxidation to ferricenium derivatives was indicated by the development of blue/green colorations.

Preparation of FcSi(^{i}Pr)$_2$H. Lithioferrocene was prepared from chloromercuriferrocene (2.00 g, 4.75 mmol) in diethyl ether (30 cm^3) and n-butyllithium (14.3 mmol) in hexane. (^{i}Pr)$_2$SiHCl (2.70 g, 17.9 mmol) was added by syringe, the mixture stirred at 35°C for 45 min, cooled and hydrolysed (*ca.* 30 cm^3 cold H_2O), and the ferrocene-containing compounds extracted into diethyl ether. The extract was dried ($MgSO_4$), filtered, and the solvent removed *in vacuo*. The residue was separated by preparative TLC (hexane) to give 2 bands. Mass and ^{1}H NMR spectroscopy showed the second band to be ferrocene and the first orange band gave diisopropylsilylferrocene, FcSi(^{i}Pr)$_2$H; yield 0.40 g (28% based on starting chloromercuriferrocene). *m/e* 301 (M^+). IR ν(Si–H), CCl_4: 2098(m) cm^{-1}. ^{1}H NMR (CCl_4): δ 4.40 (m, 10H), 1.37–0.92 (m, 14H).

Preparation of 1,1′-Fc′[SiMe$_2$H]$_2$. 1,1′-Dilithioferrocene was prepared from ferrocene (1.00 g, 5.38 mmol) in hexane (30 cm^3), n-butyllithium (10.8 mmol) and TMEDA (10.8 mmol). Me$_2$SiHCl (2.00 g, 21.2 mmol) was added by syringe. During this addition the orange suspension of 1,1′-Fc′Li$_2$ · TMEDA reacted to give a bright red/orange solution and a creamy white precipitate. The mixture was heated under reflux for 1 h to ensure complete reaction. The cooled mixture was hydrolysed (*ca.* 30 cm^3 cold H_2O) and the ferrocene containing compounds extracted into diethylether. The extract was dried ($MgSO_4$), filtered and the solvents removed *in vacuo*. The residue was separated by preparative TLC (hexane) to give 2 bands. The second band (orange), a minor product, was not investigated further. The first band (yellow/orange) was 1,1′-bisdimethylsilylferrocene, 1,1′-Fc′[SiMe$_2$H]$_2$, yield 1.43 g (88%). *m/e* 302 (M^+). IR ν(Si–H), CCl_4: 2116(m) cm^{-1}. ^{1}H NMR (CCl_4): δ 4.48 (sep, 2Si–H), 4.17 (t, 4H$_a$), 3.98 (m, 4H$_b$), 0.30 (d,

2Si–CH_3). ^{29}Si NMR (CCl_4): δ – 18.59(s). Similarly, 1,1′-Fe′[$SiPh_2H$]$_2$ was prepared from Ph_2SiHCl and 1,1′-dilithioferrocene in ether. Anal. Found: C, 74.36; 5.58. $C_{34}H_{30}FeSi_2$ calc.: C, 74.26; H, 5.51%. ^{1}H NMR ($CDCl_3$): δ 4.32 (m, 4H_a). 4.43 (m, 4H_b), 5.60 (2 Si–H), 7.55–7.79 (m, 4C_6H_5). ^{29}Si NMR: δ – 17.81 (J(Si–H), 201.8 Hz, J(Si–CH), 5.8 Hz).

Preparation of FcSi(Me$_2$)CCo$_3$(CO)$_9$. A solution of $HCCo_3(CO)_9$ (1.00 g, 2.2 mmol) and $FcSiMe_2H$ (0.50 g, 2.0 mmol) in dry toluene (*ca.* 30 cm^3) was heated under reflux for 18 min. After cooling, the solvent was removed under vacuum. The residue was dissolved in a small volume of CH_2Cl_2, and separation by preparative TLC (hexane) gave $HCCo_3(CO)_9$ (0.24 g), several minor bands that were not investigated further, and a major brown product. This was removed with CH_2Cl_2, filtered and the solvents removed *in vacuo*. Recrystallisation from hexane gave black crystals of (ferrocenyldimethylsilylmethylidinetricobaltnonacarbonyl), $FcSi(Me)_2CCo_3(CO)_9$, **1a**: 0.725 g (62% based on reacted $HCCo_3(CO)_9$). Anal. Found: C, 39.06; H, 2.55. $C_{22}H_{15}Co_3FeSiO_9$ calc.: C, 38.62; H, 2.21%. *m/e* 684 (M^+), successive loss of 9 CO follows. IR ν(CO), CCl_4: 2101w, 2052w, 2035s, 2019w. ^{1}H NMR (CCl_4): δ 4.29 (t, 2H_a), 4.15 (m, 2H_b), 4.05 (s, C_5H_5), 0.60 (s, 2Si–CH_3). ^{29}Si NMR (CCl_4): δ 2.54 (s). λ, nm (ϵ): 468 (2110), 370 (3920).

Preparation of FcSi(Ph)$_2$CCo$_3$(CO)$_9$. A solution of $HCCo_3(CO)_9$ (1.2 g, 2.7 mmol) and $FcSiPh_2H$ (1.0 g, 2.7 mmol) in dry toluene (*ca.* 30 cm^3) was heated under reflux for 30 min, during which the colour turned from purple to brown. After cooling, the solvent was removed *in vacuo*. The residue was dissolved in a small volume of CH_2Cl_2 and separated by column chromatography (silica gel). Four bands resulted. The first (purple $HCCo_3(CO)_9$) and second (yellow, identified as ferrocene by ^{1}H NMR) bands were eluted using hexane. Subsequent elution with $HCCl_3$/hexane (50/50) gave the third (brown major product) and fourth (yellow) bands. The brown solution of band three was filtered and the solvents removed *in vacuo* to give ferrocenyldiphenylsilylmethylidinetricobaltnonacarbonyl, $FcSi(Ph)_2CCo_3(CO)_9$, **1b**, as a greenish/brown solid: yield 70%. Anal. Found C, 48.72; H, 3.00. $C_{32}H_{19}Co_3FeSiO_9$ calc.: C, 47.55; H, 2.37%. Analysis for **1b** varied around these figures due to residual toluene which could not be removed without decomposing the compound. *m/e* 808 (M^+), successive loss of 9CO follows. IR ν(CO), CCl_4: 2099w, 2052vs, 2036s, 2021w. ^{1}H NMR (CCl_4): δ 7.97, 7.43 (m, 2C_6H_5), 4.58 (m, 2H_a), 4.47 (m, 2H_b), 3.90 (s, C_5H_5).

Attempted preparation of FcSi(^{i}Pr)$_2$ complexes. $HCCo_3(CO)_9$ (0.60 g, 1.4 mmol) and $FcSi(^iPr)_2H$ (0.40 g, 1.3 mmol) were dissolved in dry toluene (*ca.* 50 cm^3) and the solution heated under reflux for 90 min. Over that period of time a black precipitate was produced which showed no ν(CO) bands. A reaction between $HCCo_3(CO)_9$ (1.34 g, 3.0 mmol) and 1,1′-Fc[$Si(^iPr)_2H$]$_2$ (0.05 g, 1.2 mmol) was similarly unsuccessful.

Preparation of 1,1′-Fc′[Si(R)$_2$CCo$_3$(CO)$_9$]$_2$ (R = Me, Ph, Et). $HCCo_3(CO)_9$ (0.50 g, 1.1 mmol) and 1,1′-Fc′[$SiMe_2H$]$_2$ (0.17 g, 0.56 mmol) were dissolved in dry toluene (*ca.* 30 cm^3) and the solution heated under reflux for 30 min. By this time only a trace of $HCCo_3(CO)_9$ remained and a slight cobalt mirror had formed in the flask. After cooling, the solvent was removed *in vacuo* and the crystalline product washed with hexane until the washings were colourless. Recrystallisation from warm $CHCl_3$ gave small black/purple crystals of 1,1′-bis(dimethylsilylmethylidinetricobaltnonacarbonyl)ferrocene, 1,1′-Fc′[$Si(Me)_2CCo_3(CO)_9$]$_2$, **2a**: yield 0.494

g (74%). Anal. Found C, 34.46; H, 1.56. $C_{34}H_{20}Co_6FeSi_2O_{19}$ calc. C, 34.54; H, 1.71%. IR, ν(CO) CCl_4: 2101w, 2052vs, 2035s, 2019w. ^{1}H NMR (CCl_4): δ 4.32 (t, $4H_a$), 4.17 (m, $4H_b$), 0.65 (s, 4Si–CH_3). ^{29}Si NMR, (CCl_4): δ 2.54 (s). λ, nm (ϵ): 463 (4000), 370 (7880). **2a** is stable as a solid in the presence of water and air but decomposes slowly in solution.

Analogous reactions between $HCCo_3(CO)_9$ and 1,1′-Fc′$[SiR_2H]_2$ (R = Ph, Et) gave red–brown 1,1′-bis(diphenylsilylmethylidinetricobaltnonacarbonyl)ferrocene, 1,1′-Fc′$[Si(Ph)_2CCo_3(CO)_9]_2$ **2b**, yield 75%, and reddish black micro-crystalline 1,1′-bis(diethylsilylmethylidinetricobaltnonacarbonyl)ferrocene. 1,1′-Fc′$[Si(Et)_2CCo_3(CO)_9]_2$, **2c**, yield 60%. **2b**: Anal. Found: C, 46.21; H, 2.75. $C_{54}H_{28}Co_6FeSi_2O_{18}$ calc.: C, 45.34; H, 1.97. Analyses for this compound, like those for **1b**, were variable due to residual toluene being present even in the crystalline material. *m/e* 1430 (M^+). IR, ν(CO), CCl_4: 2099w, 2053vs, 2036s, 2021w. ^{1}H NMR (CCl_4): δ 7.96, 7.44($4C_6H_5$), 4.09 (s, $4H_a$), 4.00 (s, $4H_b$). ^{29}Si NMR (CCl_4): δ 2.54(s). λ, nm (ϵ): 460 (3770), 375 (7740). **2c**: Anal. Found: C, 36.32; H, 2.08. $C_{38}H_{28}Co_6FeSi_2O_{18}$ calc.: C, 36.84; H, 2.28%. IR ν(CO), CCl_4: 2099w, 2052vs, 2035s, 2018w. ^{1}H NMR (CCl_4): δ 4.32 (s, $4H_a$), 4.10 (s, $4H_b$), 1.52–0.53 (m, $4C_2H_5$).

Preparation of 1,1′-Fc′[Si(Me)$_2$CCo$_3$(CO)$_9$][SiMe$_2$H]. $HCCo_3(CO)_9$ (50 mg, 0.11 mmol) and 1,1′-Fc′$[SiMe_2H]_2$ (34 mg, 0.11 mmol) were dissolved in dry toluene (20 cm^3) and the solution heated under reflux for *ca.* 5 min. Over that time TLC showed that both starting materials had been consumed, and the solution had gone from a purple to a brown colour. After cooling, the solvent was removed, the residue dissolved in a small volume of CH_2Cl_2 and separated by preparative TLC (silica gel, hexane). Four bands resulted. The second band (brown, R_f *ca.* 0.35) was stripped from the plates with dry diethyl ether, filtered and the solvent removed under vacuum to give a red–brown solid 1,1′-Fc′$[Si(Me)_2CCo_3(CO)_9][SiMe_2H]$ (**3**) (1-dimethylsilylmethylidinetricobaltnonacarbonyl-1′-dimethylsilylferrocene): yield 27 mg (33% based on starting $HCCo_3(CO)_9$). *m/e* 742 (M^+), successive loss of 9 CO follows. IR ν(CO) (hexane): 2101m, 2052s, 2037vs, 2021m cm^{-1}. ^{1}H NMR ($CDCl_3$): δ 4.47 (sep, J(H–H) = 13 Hz, Si–H), 4.37 (s, 4H, Fc), 4.23 (s, 2H, Fc), 4.27 (s, 2H, Fc), 0.71 (s, 6H, 2Si–CH_3), 0.34 (d, 6H, 2Si–CH_3, J(H–H) = 13 Hz). ^{13}C NMR ($CDCl_3$): δ 199.8 (CO), 73.6 (2C, Fc), 73.3 (2C, Fc), 71.9 (2C, Fc), 71.8 (2C, Fc), 2.0 (s, 2C, 2Si–CH_3), 3.0 (s, 2C, 2Si–CH_3). ^{29}Si NMR (CCl_4): δ −18.44 (s, $Si(CH_3)_2H$), 2.62 ($Si(CH_3)_2CCo_3(CO)_9$). λ, nm (ϵ): 468 (1730), 375 (3170). This compound is extremely labile converting to **2a** and an uncharacterised black solid on standing.

Preparation of Fc[Si(Me)$_2$CCo$_3$(CO)$_{9-n}$L$_n$] and 1,1′-Fc[Si(Me)$_2$CCo$_3$(CO)$_{9-n}$-L$_n$][Si(Me)$_2$CCo$_3$(CO)$_{9-m}$L$_m$] [26]*

(a) Thermal reaction. Typically, the appropriate silyl-cluster (*ca.* 0.03 mmol) and the ligand (> 1.0 mmol excess) were dissolved in a mixture of hexane (20 cm^3) and CH_2Cl_2 (5 cm^3) and the purple solutions heated under reflux for 20 min by which time the solutions became yellow to brown in colour. Only a trace amount of the starting cluster remained. The solvent was stripped *in vacuo* and the residue

* Reference number with an asterisk indicates a note in the list of references.

dissolved in the mimimum amount of CH_2Cl_2. Preparative TLC (silica gel, hexane: CH_2Cl_2) separated the products in ascending order of substitution. Recrystallisation rarely gave pure crystalline solids and most products could only be obtained as orange–brown/green oils or impure solids. This is common for phosphine derivatives of these clusters and there was no doubt that phosphine loss and uptake of adventitious CO took place during purification; this was readily apparent from TLC and spectroscopic analysis of 'pure' material. Characterisation, which in all cases is unequivocal, rested mainly on mass spectra and spectroscopic data. **4**[1], L = PPh_3: IR, ν(CO), CCl_4: 2070m, 2037s, 2022sh, 2012s, 2002sh, 1902vw, 1875m, 1857m. ^{1}H NMR (CCl_4): δ 7.37, 7.30 (m, $3C_6H_5$), 4.27 (m, $2H_a$), 4.13 (m, $2H_b$), 3.98 (s, 5H), 0.42 (s, $2CH_3$). Fc:Me:Ph, 9:6:15. **5**[1], L = PCy_3. Anal. Found: C, 50.62; H, 5.84. $C_{37}H_{48}Co_3FeSiO_8P$ calc.: C, 50.02; H, 5.17%. IR ν(CO), CCl_4: 2065m, 2032s, 2006s, 1996sh, 1898w, 1868m, 1845m. ^{1}H NMR (CCl_4): δ 4.32 (m, $2H_a$), 4.17 (m, $2H_b$), 4.00 (s, C_5H_5), 2.52–0.79 (m, $3C_6H_{11}$), 0.37 (s, $2CH_3$). Fc:Me:Cy, 9:6:33. **6**[1], L = $P(OMe)_3$: IR ν(CO), CCl_4: 2079m, 2037s, 2019s, 2002sh, 1895w, 1876w, 1864w; ^{1}H NMR: δ 4.25 (m, $2H_a$), 4.18 (m, $2H_b$), 4.05 (s, C_5H_5), 3.66 (d, J(H–P) = 18 Hz, $3OCH_3$), 0.53 (s, $2CH_3$). Fc:Me:OMe, 9:6:9. **6**[2]: IR ν(CO) CCl_4: 2053w, 2006w, 1995s, 1987sh, 1888w, 1854m, 1846sh; ^{1}H NMR (CCl_4): δ 4.25 (m, $2H_a$), 4.17 (m, $2H_b$), 3.93 (s, C_5H_5), 3.66 (d, J(H–P) 16 Hz, 6 OCH_3), 0.32 (s, $2CH_3$). Fc:Me:OMe, 9:6:18. **7**[1], L = $P(OPh)_3$: IR ν(CO), CCl_4: 2083w, 2040sh, 2031sh, 2020s, 2004m, 1861mw. **7**[2]: IR ν(CO), CCl_4: 2041w, 2006s, 1995s, 1981sh, 1882w, 1846m, 1834m. ^{1}H NMR: δ 7.42–6.75 (m, 9 OPh), 4.09 (m, $2H_a + 2H_b$), 3.87 (s, C_5H_5), 0.37 (s, $2CH_3$). The following ν(CO) data are typical of substituted complexes from 1,1′-Fc′ clusters, other data are available from the authors. **8**[1, 0], L = PPh_3: ν(CO) CCl_4: 2100m, 2075sh, w, 2070m, 2052vs, 2036vs, 2013s 1876m, 1857m. ^{1}H NMR (CCl_4): δ 7.90–71.3 (m, 3Ph), 4.30 (m, $4H_a$), 4.17 (m, $4H_b$), 0.67 (s, $2CH_3$), 0.45 (s, $2CH_3$). **8**[1, 1]: ν(CO) CCl_4: 2075w, 2070m, 2038s, 2023m, 2012s, 1875m, 1857m. ^{1}H NMR: δ 8.03–7.23 (m, 6Ph), 4.28 (m, $4H_a$), 4.15 (m, $4H_b$), 0.45 (s, $4CH_3$). **9**[2, 2], L = $P(OMe)_3$: ν(CO) CH_2Cl_2: 2051m, 2004s, 1988s, 1887vw, 1849m. **10**[0, 1], L = $P(OPh)_3$: 2100m, 2083w, 2052vs, 2035vs, 2020m, 1860w. **10**[0, 2]: 2100w, 2065sh, 2052vs, 2035vs, 2018vs, 2002vs, 1983sh, 1896w, 1860m. **10**[0, 3]: 2100m, 2051vs, 2036vs, 2019m, 2005m, 1849w. **10**[1, 2]: 2083m, 2065m, 2041s, 2018s, 2003s, 1922w, 1853m. **10**[2, 2]: 2064, 2058m, 2018s, 2002s, 1986w, 1860. **10**[2, 3]: 2064sh, 2056m, 2041m, complex envelope follows. **10**[3, 3]: 2041m, complex envelope.

(b) Electron induced reactions. The appropriate silyl-cluster and ligand were dissolved in dry THF (2 cm^3). Two drops of a THF solution of Na–BPK were added with stirring, and within seconds a quantitative conversion to the substituted derivative occurred. Workup was as for the thermal reactions.

Chemical oxidations

Typically, on adding $AgPF_6$ (0.15 mmol) to a stirred solution of purple **1a** (0.10 g, 0.14 mmol) in CH_2Cl_2 (*ca.* 25 cm^3), the solution rapidly changed to a yellow/brown colour. The reaction was monitored by IR and deemed complete when the band at 2101 cm^{-1} disappeared; this took *ca.* 2 min. The solution was filtered and the solvent removed slowly at 273 K. Black micro-crystalline $[FcSi(Me)_2CCo_3(CO)_9]^+$–$PF_6^-$, (**1a**$^+$) resulted, ($\nu$(CO) CH_2Cl_2: 2105w, 2056s, 2043s, 2024w, paramagnetic. This compound was stable when stored as a solid.

Table 1

Crystal data, data collection and refinement of **2a**

Crystal data		Data collection and refinement	
Formula	$C_{34}H_{20}O_{18}Si_2FeCo_6$	Diffractometer	Hilger and Watts
Formula weight (g mol^{-1})	1182.15	Temperature (K)	293 ± 2
Crystal system	triclinic	Radiation	Mo-K_α (λ = 0.71069 Å)
Space group	$P\bar{1}$ (No. 2) [27]	Scan type	(ω–2θ)
a (Å)	8.675(5)	Data limits	$0 < 2\theta < 42°$
b (Å)	17.20(1)	Reflections measured:	$\pm h, \pm k, l$
c (Å)	8.661(9)	Crystal decay [a]	< 2%
α (deg)	90.86(5)	Absorption correction	analytical
β (deg)	114.90(5)	Transmission	0.673 (maximum)
γ (deg)	110.63(5)		0.436 (minimum)
V (Å^3)	1077	Total observed data	2034
D_M (g cm^{-3})	1.82 (flotation)	Unique data	1197 ($I > 2\sigma I$)
D_C (g cm^{-3})	1.82	Number of variables	198
Z	1	$R(\Sigma \lvert\lvert F_o \rvert - \lvert F_c \rvert / \lvert F_o \rvert)$	0.0698
Crystal size (mm)	0.31 × 0.35 × 0.15	$R_w[\Sigma w(\Delta F)^2 / \Sigma w F_o^{2-}]^{1/2}$	0.0711
μ(Mo-K_α) (cm^{-1})	28.0	w	$[0.7162/(\sigma^2 F + 0.000494F^2)]$

[a] Standard reflections (0 −6 0) (−3 0 0) (−2 0 2) measured after every 100 reflections.

Similar procedures were used to prepare black **2a**$^{+\cdot}$ ν(CO) CH_2Cl_2: 2105w, 2058s, 2043s, 2024w), **4**[1]$^{+\cdot}$ (ν(CO)(CH_2Cl_2), 2078m, 2039s, 2018s, 2005sh, 1904vw, 1868m), **5**[1]$^{+\cdot}$ (ν(CO)(CH_2Cl_2), 2070m, 2037s, 2010s, 1999sh, 1898vw, 1870m, 1856m), **6**[1]$^{+\cdot}$ (ν(CO)(CH_2Cl_2): 2083m, 2041s, 2025s, 1977vw and **6**[2]$^{2+\cdot}$ (ν(CO)(CH_2Cl_2): 2111w, 2068s, 2039w, sh, 2024w, sh, 2006vw, sh, 1998vw, sh).

Crystal structure determination of ***2a***

Crystals of **2a**, prepared as described previously, were grown from $CHCl_3$ solutions and a purple–black block was selected for data collection. Precession photography, using Cu-K_α radiation indicated a triclinic system, and the space group was confirmed as $P\bar{1}$ (No. 2) [27] by the success of the structure refinement. Data were collected at 293 ± 2 K on a Hilger and Watts, four circle, fully automated diffractometer. The cell dimensions and orientation matrices were calculated from 15 accurately centred reflections. The crystals obtained were not of good quality. The crystal used for data collection showed widths at half height for typical intense, low-angle reflections of 0.650 and exhibited two distinct maxima in ω-scans, however the data obtained from this sample proved adequate for the solution of the structure. Reflection data were processed using HILGOUT [28*]. Relevant details of the crystal, data collection, solution and refinement are summarised in Table 1. The positions of the cobalt atoms were determined by Patterson methods and, in the centrosymmetric space group with $Z = 1$, the Fe atom was constrained to lie on the special position $\frac{1}{2}$,0,0 (d for $P\bar{1}$ in the Wyckoff notation) [27]. The remaining non-hydrogen atoms were found in subsequent difference Fourier, least-squares refinement cycles using the program SHELX-76 [29]. The function minimised was $\Sigma w(\lvert F_o \rvert - \lvert F_c \rvert)^2$, with scattering factors for the

Table 2

Final positional and equivalent thermal parameters for **2a**

Atom	x	y	z	U_{eq} / U_{11}
Fe	0.5000	1.0000	0.0000	0.042
C(1)	0.546(3)	1.106(1)	−0.111(3)	0.037(5)
C(2)	0.633(3)	1.129(1)	0.074(3)	0.050(6)
C(3)	0.764(3)	1.089(1)	0.155(3)	0.047(6)
C(4)	0.759(3)	1.046(1)	0.010(3)	0.055(7)
C(5)	0.631(3)	1.053(2)	−0.146(3)	0.058(7)
Si	0.3767(7)	1.1418(4)	−0.2761(8)	0.038
C(6)	0.258(4)	1.067(2)	−0.487(3)	0.079(8)
C(7)	0.198(3)	1.148(1)	−0.214(3)	0.044(6)
Cap	0.517(3)	1.253(1)	−0.290(3)	0.038(5)
Co(1)	0.4613(4)	1.3130(2)	−0.4785(4)	0.043
Co(2)	0.6107(3)	1.3606(2)	−0.1627(4)	0.038
Co(3)	0.7512(4)	1.2954(2)	−0.2937(4)	0.037
C(11)	0.228(4)	1.305(2)	−0.516(3)	0.065(7)
O(11)	0.084(2)	1.296(1)	−0.544(3)	0.104
C(12)	0.386(4)	1.240(2)	−0.657(4)	0.066(8)
O(12)	0.346(3)	1.189(2)	−0.774(3)	0.116
C(13)	0.557(3)	1.413(2)	−0.544(3)	0.064(7)
O(13)	0.608(3)	1.470(1)	−0.598(3)	0.130
C(21)	0.714(3)	1.346(2)	0.050(4)	0.051(7)
O(21)	0.781(2)	1.340(1)	0.193(3)	0.081
C(22)	0.417(3)	1.369(1)	−0.143(3)	0.047(6)
O(22)	0.304(2)	1.379(1)	−0.121(3)	0.104
C(23)	0.751(3)	1.472(2)	−0.146(3)	0.060(7)
O(23)	0.832(2)	1.538(1)	−0.150(3)	0.096
C(31)	0.730(3)	1.210(2)	−0.425(3)	0.050(6)
O(31)	0.716(2)	1.153(1)	−0.510(3)	0.084
C(32)	0.900(3)	1.276(1)	−0.100(3)	0.035(5)
O(32)	1.003(2)	1.264(1)	0.023(2)	0.070
C(33)	0.919(3)	1.392(2)	−0.333(3)	0.053(7)
O(33)	1.016(2)	1.451(1)	−0.341(3)	0.088

Co and Fe atoms and corrections for anomalous dispersion taken from the usual compilation [30]. Absorption corrections were applied [31*] and the Fe, Co, and Si atoms together with the oxygen atoms of the carbonyl ligands assigned anisotropic temperature factors. Hydrogen atoms were included in calculated positions with d(C–H) 0.98 Å, a weighting scheme based on counting statistics was introduced and this structural model converged with $R = 0.0698$ and $R_w = 0.0711$ for a data to parameter ratio of 6.0. A final difference Fourier synthesis showed a number of peaks of intensity 1.0–0.8 eÅ^{-3} in the vicinity of the cobalt triangle. Final positional and equivalent thermal parameters for **2a** are given in Table 2 with selected bond length and angle data in Table 3. A full table of bond lengths and angles, and tables of anisotropic temperature factors have been deposited with the Cambridge Crystallographic Data Centre and a list of observed and calculated structure factor amplitudes and mean-plane data for **2a** is available from the authors (J.S.).

Table 3

Selected bond lengths (Å) and angles (deg) for **2a**

Bond lengths			
Fe–C(1)	2.07(2)	Co(1)–C(11)	1.87(3)
Fe–C(2)	2.05(2)	Co(1)–C(12)	1.71(3)
Fe–C(3)	2.07(2)	Co(1)–C(13)	1.85(3)
Fe–C(4)	2.06(2)	Co(2)–Co(3)	2.474(4)
Fe–C(5)	2.06(2)	Co(2)–C(21)	1.75(3)
C(1)–C(2)	1.43(3)	Co(2)–C(22)	1.82(2)
C(1)–C(5)	1.46(3)	Co(2)–C(23)	1.83(3)
C(1)–Si	1.86(2)	Co(3)–C(31)	1.75(3)
C(2)–C(3)	1.47(3)	Co(3)–C(32)	1.76(2)
C(3)–C(4)	1.41(3)	Co(3)–C(33)	1.93(3)
C(4)–C(5)	1.38(3)	C(11)–O(11)	1.11(3)
Si–C(6)	1.86(3)	C(12)–O(12)	1.17(3)
Si–C(7)	1.88(2)	C(13)–O(13)	1.12(3)
Si–Cp(1)	1.91(2)	C(21)–O(21)	1.15(3)
Cap–Co(1)	1.93(2)	C(22)–O(22)	1.14(2)
Cap–Co(2)	1.85(2)	C(23)–O(23)	1.12(3)
Cap–Co(3)	1.92(2)	C(31)–O(31)	1.16(3)
Co(1)–Co(2)	2.456(4)	C(32)–O(32)	1.15(2)
Co(1)–Co(3)	2.478(4)	C(33)–O(33)	1.10(3)
Bond angles			
Fe–C(1)–Si	129(1)	Co(3)–Co(1)–C(13)	99.9(7)
C(2)–C(1)–C(5)	104(2)	Co(1)–Co(2)–Co(3)	60.3(1)
C(2)–C(1)—Si	129(2)	Cap–Co(2)–Co(1)	50.7(6)
C(5)–C(1)–Si	126(2)	Cap–Co(2)–Co(3)	50.1(6)
C(1)–C(2)–C(3)	111(2)	Co(1)–Co(2)–C(21)	152.5(8)
C(2)–C(3)–C(4)	103(2)	Co(1)–Co(2)–C(22)	98.6(7)
C(3)–C(4)–C(5)	112(2)	Co(1)–Co(2)–C(23)	99.8(8)
C(1)–C(5)–C(4)	108(2)	Co(3)–Co(2)–C(21)	100.0(8)
C(1)–Si–C(6)	109(1)	Co(3)–Co(2)–C(22)	153.6(7)
C(1)–Si–C(7)	112.7(9)	Co(3)–Co(2)–C(23)	98.0(8)
C(1)–Si–Cap	106.0(9)	Co(1)–Co(3)–Co(2)	59.5(1)
C(6)–Si–C(7)	108(1)	Cap–Co(3)–Co(1)	50.0(6)
C(6)–Si–Cap	111(1)	Cap–Co(3)–Co(2)	47.9(6)
C(7)–Si–Cap	108.4(9)	Co(1)–Co(3)–C(31)	100.6(7)
Si–Cap–Co(1)	129(1)	Co(1)–Co(3)–C(32)	151.9(6)
Si–Cap–Co(2)	135(1)	Co(1)–Co(3)–C(33)	97.6(6)
Si–Cap–Co(3)	129(1)	Co(2)–Co(3)–C(31)	149.2(7)
Co(1)–Cap–Co(2)	81.0(8)	Co(2)–Co(3)–C(32)	96.5(6)
Co(1)–Cap–Co(3)	80.3(8)	Co(2)–Co(3)–C(33)	102.7(7)
Co(2)–Cap–Co(3)	82.0(8)	Co(1)–C(11)–O(11)	175(3)
Co(2)–Co(1)–Co(3)	60.2(1)	Co(1)–C(12)–O(12)	175(3)
Cap–Co(1)–Co(2)	48.2(6)	Co(1)–C(13)–O(13)	173(3)
Cap–Co(1)–Co(3)	49.7(6)	Co(2)–C(21)–O(21)	176(2)
Co(2)–Co(1)–C(11)	95.6(8)	Co(2)–C(22)–O(22)	175(2)
Co(2)–Co(1)–C(12)	151.2(9)	Co(2)–C(23)–O(23)	173(3)
Co(2)–Co(1)–C(13)	100.2(8)	Co(3)–C(31)–O(31)	178(2)
Co(3)–Co(1)–C(11)	148.8(8)	Co(3)–C(32)–O(32)	176(2)
Co(3)–Co(1)–C(12)	98.0(9)	Co(3)–C(33)–O(33)	173(2)

Results and discussion

Preparation of $FcSi(R)_2CCo_3(CO)_9$ and 1,1'-$Fc'[Si(R)_2CCo_3(CO)_9]_2$

Attachment of the $CCo_3(CO)_9$ cluster fragment to silicon is readily achieved utilising the hydrogen elimination reaction between a silicon hydride and $HCCo_3(CO)_9$ [12]. This method was applied successfully to both mono- and bis-silylferrocene systems to give good yields of compounds with one (eq. 1) or two (eq. 2) cluster units per ferrocene moiety.

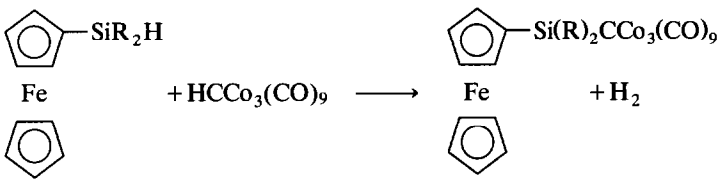

(1)

Compound **1a**: R = Me; **1b**: R = Ph

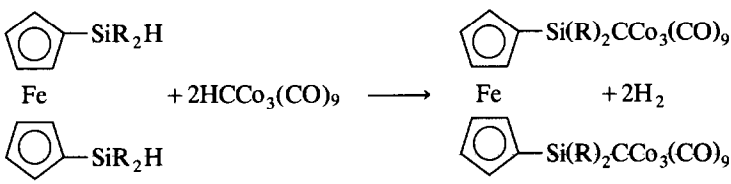

(2)

Compound **2a**: R = Me; **2b**: R = Ph; **2c**: R = Et

It has been noted previously that steric crowding at the silicon centre can drastically limit the efficacy of this preparative route [32]. In this work, attempts to prepare the compounds with ^{i}Pr substituents at silicon were unsuccessful as a result of unacceptable non-bonded interactions between the silyl substituents and the equatorial carbonyl ligands of the cluster unit.

Isolation of the unstable complex **3** (eq. 3) from a reaction with a 1:1 silane:cluster stoichiometry confirmed that the hydrogen elimination reaction occurs in a stepwise fashion. Other intermediates for R = Ph, Et were identified spectroscopically but they rapidly formed the respective complexes **2b** or **2c** on workup together with a black solid which has not been characterised.

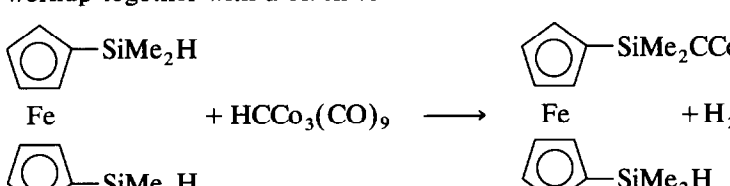

(3)

3

The ν(CO) profiles for **1**, **2** and **3** are similar to those of other $-CCo_3(CO)_9$ compounds [33] and the ν(CO) A_{1-sym} band does not vary greatly with changes to the silicon substituents. Hence transmission of electron density via the capping carbon atom of the cluster is insensitive to changes at silicon. The ^{1}H NMR spectra are readily interpreted. For instance, in **1a**, the unsubstituted cyclopentadienyl ring resonance is close to that of ferrocene, while the substituted ring proton

Table 4

^{29}Si NMR spectra of some ferrocenylsilane complexes, 1,1'-Fc'[R][R']

R	R'	δ (ppm)		
		$SiMe_3$	SiR_2H	$Si(R)_2CCo_3(CO)_9$
$SiMe_3$	H	−3.64		
$SiMe_2H$	$SiMe_2H$		−18.59	
$SiPh_2H$	$SiPh_2H$		−18.02	
$SiMe_2CCo_3(CO)_9$	H			2.54
$SiMe_2CCo_3(CO)_9$	$SiMe_2H$		−18.44	2.62
$SiMe_2CCo_3(CO)_9$	$SiMe_2CCo_3(CO)_9$			2.54

resonances are shifted to lower field commensurate with electron withdrawal by the $Si(Me)_2CCo_3$ moiety [34]. However the observed deshielding is much less than that observed in $FcCCo_3(CO)_9$ [4], pointing to an attenuation of the electron withdrawing effect of the cluster unit by the interpolated silicon atom. The ^{1}H NMR spectrum of **2a** is similar, allowing for the absence of a resonance due to an unsubstituted ring. The alpha and beta protons of the $Si(Me)_2CCo_3$ substituted ring are also resolved in the spectrum of **3** in contrast to those from the ring with the Me_2SiH substituent. All compounds show the anticipated two bands at *ca.* 450–500 nm and *ca.* 370 nm [4,35], in their visible spectra (see Experimental). The extinction coefficients for each band due to the diclusters, **2a** and **2b**, are approximately twice those for the monocluster complex, **1a** and **3**, indicating that the transitions must be localised on the cluster core. There is no marked red shift in the *ca.* 370 nm band on ferrocenyl substitution at silicon, in contrast to the situation in $FcCCo_3(CO)_9$, where the reduction in energy of transitions from the π-(Co_3C_{apical}) bonding levels was ascribed to a significant π-interaction between the Fc and cluster moieties [4].

Silicon-29 NMR proved to be a valuable routine technique in the characterisation of these derivatives. Several factors (low natural abundance, small magnetogyric ratio, negative NOE and long spin-relaxation times) have limited the usefulness of this technique in the past [36] but DEPT pulse sequences [20] gave greatly enhanced signals in the case of the cluster compounds. Electronic effects do not always influence the ^{29}Si chemical shift in an additive fashion because geometry, steric interactions and π-bonding may be equally important [37]. Table 4 gives the data for ferrocenylsilanes and their cluster analogues. There is a remarkable consistency and additivity in the ^{29}Si chemical shift for the cluster derivatives. Thus the chemical shift for the pairs **1a/2a** and **1b/2b** are identical; further the chemical shifts for **3** are a combination of the values for the uncoordinated ferrocenylsilane and **1a**. These data negate any suggestions of steric influence on the chemical shift (the structure of **2a**, *vide infra*, shows that the silicon atom is still tetrahedrally coordinated) and show clearly that the ferrocene moiety is isolating the two silicon centres. Substitution at silicon by the electron-donating ferrocene unit results in the expected upfield shift from the parent silane R_3SiH [38], whereas substitution by the tricobalt cluster at the ferrocenyl silane gives a large downfield shift. It is easy to attribute this downfield shift to the electron-withdrawing properties of the Co_3C core, this electronic effect of the cluster is well-docu-

mented [39–41], but it is important to note that the chemical shift is considerably downfield from silylmetal carbonyls and more akin to silylmercury derivatives.

Spectroscopic data confirm that derivatives of **1a** and **2a** with one phosphine or phosphite ligand per cluster unit could be prepared in quantitative yield using electron transfer catalysed (ETC) techniques [42,43]. Termination of the ETC cycle after the substitution by one Lewis base is due to reduced catalytic efficiency, a well-documented facet of ETC nucleophilic substitution [44]. However, the synthetic advantages of the ETC method was apparent when compared with the non-selective thermal reactions with phosphites.

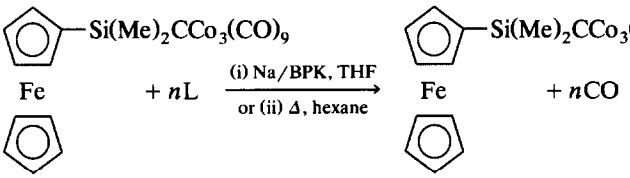

(4)

Compound	**4**[n]	**5**[n]	**6**[n]	**7**[n]
L	PPh_3	PCy_3	$P(OMe)_3$	$P(OPh)_3$
(i) n	1	1	1	1
(ii) n	1	1	1,2	1,2,3

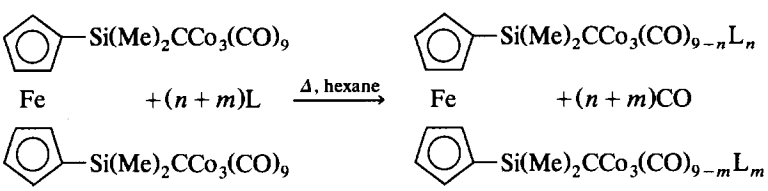

(5)

Compound	**8**[m,n]	**9**[m,n]	**10**[m,n]
L	PPh_3	$P(OMe)_3$	$P(OPh)_3$
m	0,1	2	0; 1; 2; 3
n	1,0	2	1,2,3; 2,3; 2,3; 3

For example the reaction of **2a** with excess $P(OPh)_3$ resulted in the formation of *eight* of the nine possible products (assuming that a maximum of three CO ligands per cluster unit can be substituted) whereas under similar conditions with $P(OMe)_3$ only one derivative **9**[2, 2] separated from the reaction. It is likely that the randomness of the product distribution in the thermal reactions is, at least partly, due to the extreme lability of these derivatives in solution. Unfortunately, this lability also frustrated attempts to obtain analytical pure crystalline samples so identification for some derivatives, although unequivocal, rests on solution NMR and IR data. Earlier work [33,45] has conclusively demonstrated that each substitution of one carbonyl group in a tricobalt carbon entity by a phosphine or phosphite shifts the cluster symmetrical in-phase carbonyl stretching mode by 25–30 cm^{-1}, providing a simple procedure for determining stoichiometry. Furthermore, spectra of the dicluster derivatives demonstrate a common feature of ferrocene chemistry [46], namely that the iron atom acts as a buffer between the two cyclopentadienyl ligands and, to a good approximation, the spectral properties of one ring and its

substituents are unaffected by a change of substituent on the other. For example, the ν(CO) spectrum of **9**[2, 2] is identical to that of **6**[2]. With these principles in mind IR spectra of other derivatives, particularly the eight from **2a**, are readily assigned. Thus the PPh_3 derivative of **2a**, **4**[1], has the symmetrical stretching mode, $\nu(CO)_t$, at 2070 cm^{-1} (*cf.* **1a** at 2101 cm^{-1}) and that for the symmetrically substituted derivative **8**[1, 1], at 2075 cm^{-1}; on the other hand, the asymmetrical derivative, **8**[1, 0], has $\nu(CO)_t$ at 2100 and 2075 cm^{-1}. NMR data fully substantiate these assignments (see Experimental).

It is surprising that the Lewis base derivatives prepared here *all* show infrared bands attributable to carbonyl-bridged configurations, including the $n = 1$ derivatives with $L = P(OMe)_3$, $P(OPh)_3$. A carbonyl-bridging structure provides steric relief and dissipates CCo_3 core electron density by more effective $d(Co) \rightarrow \pi^*(CO)$ back-donation [45]. Except for $FcCCo_3(CO)_{9-n}L_n$ compounds [4,5], carbonyl-bridged conformations have only been observed in clusters substituted by phosphines, whereas phosphite derivatives have invariably been non-bridged [45]. In the $FcCCo_3(CO)_{9-n}L_n$ series, all but the $n = 1$ derivatives were shown to have carbonyl-bridged configurations [4,5], which could again be rationalised in terms of electron release from Fc to the cluster. While there is evidence for the $FcSi(Me)_2$–moiety acting as a net electron donor to the cluster unit, the extent of electron donation is manifestly reduced in the silicon bridged systems. Carbonyl bridging in these systems may therefore be a response to the steric congestion imposed by the equatorial substitution by bulky ligands on an already strained $FcSi(Me)_2CCo_3$ fragment. Comparison of the $\nu(CO)_{t-sym}$ bands from the IR spectra of these derivatives with those of $MeCCo_3(CO)_{9-n}L_n$ and $FcCCo_3(CO)_{9-n}L_n$ reveals that the extent of $d(Co) \rightarrow \pi^*(CO)$ back-donation varies in the order $FcCCo_3(CO)_{9-n}L_n \gg FcSi(Me)_2Co_3(CO)_{9-n}L_n \approx 1,1'\text{-}Fc'[Si(Me)_2CCo_3(CO)_{9-n}L_n]_2 > MeCCo_3(CO)_{9-n}L_n$. In the case of the directly bound Fc capping substituent, these observations could be rationalised in terms of a facile mechanism for electron donation from the Fc moiety to the cluster by delocalisation through the carbyne cap [4,9]. Clearly the extent of such donation is severely attenuated in the molecules described here.

Unexpectedly, the reaction of **2b** with phosphines and phosphites gave products *without* a ferrocene moiety; ferrocene is a by-product. These products are under investigation but it is suggested that steric congestion in the derivatives of **2b** forces a reductive elimination reaction resulting in cleavage of the Fc–Si bonds.

Crystal structure determination of 2a

The relative instability of the mono- and dicluster complexes with $SiPh_2$ linking the ferrocenyl and cluster fragments, our inability to synthesise the corresponding isopropyl clusters, and the extreme lability of Lewis base derivatives suggested a degree of steric crowding around the silicon atom. To investigate the minimum energy configuration of the μ-SiR_2 bridge, and to determine if there was any evidence from the solid state structure for interaction between the redox centres, an X-ray structure analysis of **2a** was undertaken. The structure consists of well-separated monomeric molecules with the closest intermolecular contact not involving H atoms being 3.02(3) Å between O(11) and O(21). Figure 1 shows a perspective view of the molecule and displays the atom numbering scheme. Selected bond length and angle data are given in Table 3.

The molecular structure of **2a** can be described as that of a ferrocene molecule with each cyclopentadienyl ring substituted in a transverse fashion by an $Si(Me)_2CCo_3(CO)_9$ moiety. The dimethylsilyl group acts as a bridge between each cyclopentadienyl ring and the capping carbon atom of a tricobalt carbon cluster. The molecule is strictly centrosymmetric with the Fe atom of the substituted ferrocenyl group located at a crystallographic centre.

The η^5-C_5H_4 rings adopt a staggered configuration with the bulky silyl-bridged cluster substituents in a *transoid* orientation which would minimise steric interactions across the ferrocene molecule. This contrasts with the structure of 1,1'-$Fc'[SiMe_2SiMe_3]_2$ [47] where the cyclopentadienyl rings are nearly eclipsed, although having the disilyl substituents on opposite sides of a plane through the Fe atom normal to the mean plane of the rings. The cyclopentadienyl rings are essentially planar with the Fe atom 1.663(2) Å from each plane. Other dimensions within the ferrocene moiety are unexceptional [48,49] with mean values of Fe–C(ring) = 2.06(1) Å and C(ring)–C(ring) = 1.43(3) Å; there is no significant variation in these C–C bond lengths. The bridging Si atom is bent out of the cyclopentadienyl ring plane, away from the Fe atom by 0.087(7) Å unlike the bis-disilyl derivative [47] where the substituent Si atoms lie in the ring plane. In the singly substituted $FcSiPh_2H$ [50], where the steric requirements of the silyl substituents are less severe, the Si atom bends out of the cyclopentadiene ring plane towards the Fe atom. The movement of the Si atom observed in **2a** clearly serves to attenuate non-bonded interactions between the ring carbon atoms and the equatorial carbonyl ligands of the cluster fragment (*vide infra*).

The tricobalt-carbon cluster unit has a distorted tetrahedral geometry. The basal cobalt triangle of the CCo_3 tetrahedron is essentially symmetrical with barely significant differences in the lengths of the Co–Co vectors. The bonds from Co(1) and Co(3) to the apical carbon atom, Cap, are normal [40], Co(1)–Cap 1.93(2) Å, Co(3)–Cap 1.92(2) Å, with the Co(2)–Cap bond marginally shorter (*ca.* 3σ) at 1.85(2) Å. This has the effect of displacing the capping carbon atom towards the Co(2)–Co(3) bond and may reduce the non-bonded interactions between the equatorial carbonyl ligands on the cluster and the cyclopentadienyl ring which binds to the bridging Si atom above the Co(2)–Co(3) bond. The location of the C_5H_4 ring with respect to the CCo_3 core is further affected by a widening of the Co(2)–Cap–Si angle to 135(1)°. The influence of interactions between the carbonyl ligands and the sterically demanding $Si(Me)_2C_5H_4Fe$ apical group is evident from the reduction of the dihedral angle between the Co(1)–Co(2)–Co(3) plane and the plane containing C(21)–Co(2)–C(22) to 27.6(8)° in comparison to 31.4(8)° for the corresponding angle involving the relatively uncluttered equatorial substituents on Co(1).

The dimethylsilyl fragment, which bridges the ferrocene and cluster portions of the molecule, binds to the apical carbon atom of the Co_3C core and to C(1) of the cyclopentadiene ring. The bonds Si–C(1), 1.86(2) Å, and Si–Cap, 1.91(2) Å, are not significantly different from those to the methyl substituents or from those reported [47,50] for other silyl substituted ferrocenes. Furthermore, the bond angles around Si do not differ markedly from the anticipated tetrahedral values. There is thus no evidence from the solid state structure to suggest any unusual electronic interaction between the cluster and ferrocene redox sites in the molecule in keeping with the electrochemical observations described later. Structural distortions that do

occur can best be ascribed to an attempt to minimise intramolecular non-bonded interactions between electronically discrete portions of the molecule.

Redox chemistry

Electrochemical data are given in Table 5 for the complexes **1a, b** and **2a, b** and some Lewis base derivatives of **1a** and **2a**. For convenience the complexes will be discussed in groupings based on the number of CCo_3 clusters per Fe unit and the degree of ligand substitution.

Complexes with one $CCo_3(CO)_9$ unit. Both representatives **1a** and **1b** undergo an electrochemically reversible one-electron oxidation and a one-electron reduction step; $E^{+/0}$, $E^{0/-}$ (CH_2Cl_2) are 0.78, −0.52 and 0.77, −0.56 V for **1a** and **1b** respectively (Fig. 2). A further irreversible multi-electron reduction occurs at more negative potentials. The close similarity of these parameters to those for the oxidation of ferrocene [23] and the reduction of other tricobalt carbon clusters [51] respectively allows their assignment to the individual redox centres, Fe and Co_3C.

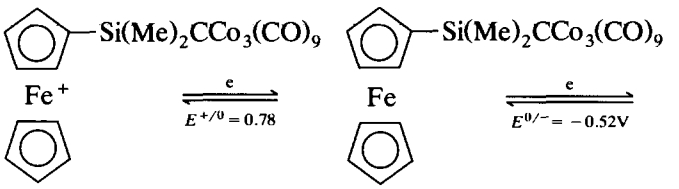

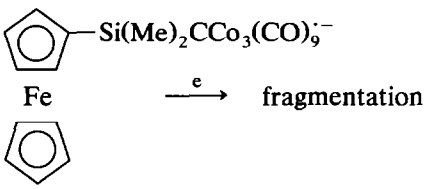

(6)

Confirmation of this assignment comes from the observation of an ESR spectrum of the radical anion **1a**$^{\cdot -}$ obtained by *in situ* reduction of **1a** in CH_2Cl_2 at 233 K, the parameters $\langle g \rangle = 2.022$ and $A_{iso} = 3.50$ mT being typical of tricobaltcarbon cluster radical anions [22,52].

In the case of **1a** the polarographic current ratio, or the comparable voltammetric peak current ratio, for the individual couples ($i(Fc^{+/0}) : i(Co_3C)^{0/-}$) is unity; that is, the electron transfer is chemically reversible. However, this ratio for **1b** is > 1 at all temperatures. As both redox centres are in the one molecule the diffusion coefficient for both electron transfer steps should be the same and thus the current equal if the oxidation of the ferrocene and reduction of the cluster redox centres are both chemically reversible. The smaller current exhibited by the $Co_3Co^{0/-}$ couple is due to fragmentation of the radical anion **1b**$^{\cdot -}$ since at all scan rates and temperatures an oxidation feature attributable to $Co(CO)_4^-$ is seen in the second and subsequent voltammetric scans of **1b**, even if the scan is reversed before the second reduction potential (usually the fragmentation of tricobaltcarbon radicals to $Co(CO)_4^-$ occurs after the second reduction step [51]). This fragmentation is not influenced by oxidation of the ferrocene moiety as the same voltammetric responses are seen if the initial sweep potential is positive or negative of $E_{1/2}(Fc^{+/0})$, or by temperature. There is no obvious explanation for the faster fragmentation of **1b**$^{\cdot -}$ on the voltammetric timescale compared to **1a**$^{\cdot -}$ although

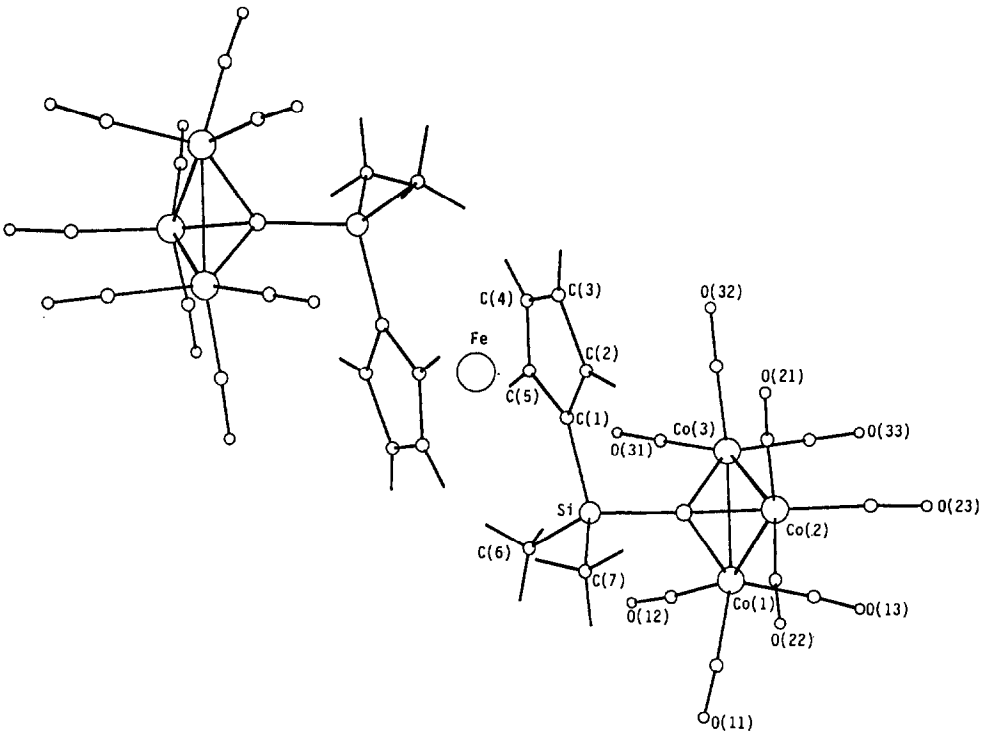

Fig. 1. Perspective view of **2a** showing the atom numbering scheme.

molecular graphics suggest that **1b** is more sterically congested; this congestion could increase upon formation of the radical anion. It may be steric crowding can facilitate a decomposition process involving the rupture of Si–C bonds (*vide supra*).

It is more difficult to oxidise the ferrocenyl moiety in these complexes than in ferrocene itself and this is reflected in the substituent parameters δ_{CCo_3} of 0.06 V (**1a**) and 0.05 V (**1b**), calculated from the $E^{+/0}$ values using the standard relationship [53]. These may be compared with $\delta_{CCo_3} = 0.09$ V obtained from data for the cluster $FcCCo_3(CO)_9$. Thus an SiR_2 group interpolated between the two redox centres mitigates the overall $-I$ effect of a $CCo_3(CO)_9$ cluster. Attenuation by the SiR_2 group of any possible electronic interaction between the redox centres is also seen in the $E^{0/-}$ data. A ferrocenyl group functions as an electron donor comparable to a methyl group, $E^{0/-}(FcCCo_3(CO)_9) = -0.60$ V, $E^{0/-}(MeCCo_3(CO)_9) = -0.61$ V but $E^{0/-}$(**1a**) $= -0.52$ V and $E^{0/-}(PhCCo_3(CO)_9) = -0.56$ V [4].

Stoichiometric oxidation of purple **1a** with Ag^I produced the brown species $[FcSi(Me)_2CCo_3(CO)_9]^+$ in which the ferrocenyl redox centre has been oxidised. Evidence for the assignment of ferrocene as the oxidation centre is indirect as the electronic transition around 617nm, typical of a ferricenium ion [46,54], was obscured by the cluster spectrum. The ν(CO) profile for the cation is the same as the parent but the bands are shifted to higher energy by *ca.* 4 cm^{-1}. This may be

compared with the shift of 12 cm^{-1} for the complex where the ferrocenyl centre is directly bound to the cluster [4].

Phosphine **4**[1], **5**[1] and phosphite **6**[1], **6**[2] derivatives also underwent the same redox processes as the parent molecules and the one-electron oxidation steps are chemically reversible at potentials close to that for the $Fc^{+/0}$ in **1a** (Table 5).

In comparison with the parent molecules it is more difficult to reduce the Co_3C moiety in these Lewis base derivatives; $E^{0/-}$ decreases by ~ 0.2 V per unit increase in n (Table 5), similar to the decrease noted with other $RCCo_3(CO)_{9-n}L_n$ derivatives [55]. Furthermore, the reduction steps are chemically irreversible at all scan rates at 293 K (Fig. 3) but in contrast to the voltammetric behaviour of **1b** chemical reversibility increases at low temperatures. It is significant that the diffusion and peak currents for the reduction wave on mercury, glassy carbon and platinum electrodes are *greater* than unity relative to the internal $Fc^{+/0}$ couple. Furthermore, on repeat scans, new waves appear corresponding to the couple $E^{0/-}$[**1a**] but those due to $Co(CO)_4^-$ (*cf.* **1b**) are absent. This electrochemical behaviour is similar to that observed for other tricobalt derivatives [44,54]. It is indicative of an $\vec{E}\vec{C}\vec{E}$ mechanism in which the one-electron transfer to the substituted cluster causes an increase in the lability of the ligands, leading ultimately to ligand dissociation and a fast electron transfer to the product of ligand dissociation [44]. The importance of this $\vec{E}\vec{C}\vec{E}$ mechanism in the electrochemistry of **4**[1]–**6**[1] is a reflection of the facile lability of both the neutral (*vide supra*) and the radical anions.

The principal redox reactions occurring in the $n = 1$ system are summarised in eq. 7.

$$\begin{array}{ccccc} FcSi(R)_2CCo_3(CO)_8L & \overset{E_r,\,e}{\rightleftharpoons} & FcSi(R)_2CCo_3(CO)_8L^- & \underset{CO/L}{\overset{-L}{\rightleftharpoons}} & \\ & & & & \text{fast} \\ \Big\| e & & & & \\ FcSi(R)_2CCo_3(CO)_8L^+ & & & & \end{array}$$

$$FcSi(R)_2CCo_3(CO)_8^- \underset{E_r^1 \geq E_r}{\overset{E_r^1,\,e}{\rightleftharpoons}} FcSi(R)_2CCo_3(CO)_8^{2-} \quad (7)$$

*Complexes with two $CCo_3(CO)_9$ units (**2a**, **2b**).* The redox behaviour of **2a** and **2b** is a superposition of one oxidisable ferrocene centre and two equivalent reducible cluster centres, which are non-interacting in an electrochemical sense [56] (Fig. 4, Table 5). Both redox processes are chemically reversible for **2a** and the ratio of the diffusion currents $i^{+/0}:i^{0/-}$ is 0.5 as expected.

Confirmation that the two cluster units are acting independently was obtained from the weak ESR spectrum obtained by the *in situ* reduction of **2a** at 293 K in CH_2Cl_2, the parameters $\langle i \rangle = 2.023$ and $A_{iso} = 3.50$ mT are almost identical to those for $\mathbf{1a}^{\cdot -}$. From this evidence it would appear that there are no cooperative interactions between the two cluster centres through the 1,1′-$Fc'(SiR_2)_2$ unit, with the silicon atoms of the μ-SiR_2 bridges effectively insulating the redox centres in the molecule. The voltammetric responses for the first reduction wave of **2b** are similar to **1b** in that fragmentation to $Co(CO)_4^-$ is seen after the formation of the radical anion. Chemical oxidation of **2a** produced the black cation 1,1′-

Table 5

Electrochemical data for some ferrocenyl silyl derivatives of the tricobalt carbon cluster

	Reduction		Oxidation	
	$E_{1/2}$ (V)	$E_{1/4}-E_{3/4}$ (mV)	$E_{1/2}$ (V)	$E_{1/4}-E_{3/4}$ (mV)
(a) Mercury electrode [a]				
1a	−0.52	60	0.78	56
	−1.22	–		
1b	−0.56	58	0.77	65
	−1.35	–		
2a	−0.63	70	0.78	60
	−1.31	–		
2b	−0.62	90	0.83	60
	−1.30	–		
4[1]	−0.83	70	0.74	60
5[1]	−0.83	58	0.74	60
6[1]	−0.85	65	0.71	58
6[2]	−1.09	105	0.74	90
8[1, 0]	−0.58	60	0.79	65
	−0.81	80		
	−1.29	–		
8[1, 1]	−0.84	100	0.77	64
10[2, 0]	−0.56	55	0.65	–
	−0.90	50	0.77	–
	−1.10	–		
10[2, 1]	−0.81	70	0.55	80
	−0.99	90	0.73	65
			0.93	–

	Reduction				Oxidation			
	E_{pc} (V)	E_{pa} (V)	$\lvert\Delta E_p\rvert$ (mV)	i_{pc}/i_{pa}	E_{pc} (V)	E_{pa} (V)	$\lvert\Delta E_p\rvert$ (mV)	i_{pc}/i_{pa}
(b) Platinum electrode [b,f]								
1a	−0.60	−0.48	120	1	0.70	0.83	120	1
1b [c]	−0.73	−0.51	220	1	0.73	0.89	160	1
2a	−0.74	−0.57	170	1	0.70	0.86	160	1
2b [d]	−0.74	−0.49	255	1	0.77	0.91	140	1
4[1]	−0.90	–	–	Irrev	0.62	0.84	220	1
	–	−0.52	–	–				
5[1]	–	–	–	Irrev	0.65	0.84	220	1
6[1]	−1.01	–	–	Irrev	0.55	0.88	330	1
	–	−0.56	–	–				
6[2]	−1.2	–	–	–	0.57	0.89	320	1
	−1.4			Irrev				
8[1, 0]	−0.68	−0.52	160	~1	0.71	0.86	150	1
	−0.92	−0.76	160	Irrev				
	−1.29	–	–	Irrev				
8[1, 1]	(−0.65) [e]	−0.53	–	–	0.65	0.84	190	1
	−1.00	–	–	Irrev				
10[2, 0]	−0.64	−0.53	110	1	0.64	0.78	140	1
	(−0.82) [e]	–	–	Irrev	1.23	–	–	Irrev
	−1.05	–	–	Irrev	1.43	–	–	Irrev
10[2, 1]	−0.67	−0.59	80	1	0.66	0.79	130	1
	−0.86	−0.75	110	Irrev	–	1.23	–	Irrev
					1.27	1.40	130	Irrev

[a] Drop time, 0.5 s; scan rate, 20 mV s^{-1}; in CH_2Cl_2. [b] Scan rate, 200 mV s^{-1}; in $CHCl_2$; ΔE_p depends on the treatment of the electrode. [c] $i_{pc}/i_{pa}(Fc) > i_{pc}/i_{pa}(CCo_3/(CO)_9)$ at all temperatures. [d] Cluster reduction not reversible at slow speeds. [e] In second and succeeding scans. [f] 'First' reduction of the $-CCo_3(CO)_{9-n}L_n$ groups involved ~2 electrons.

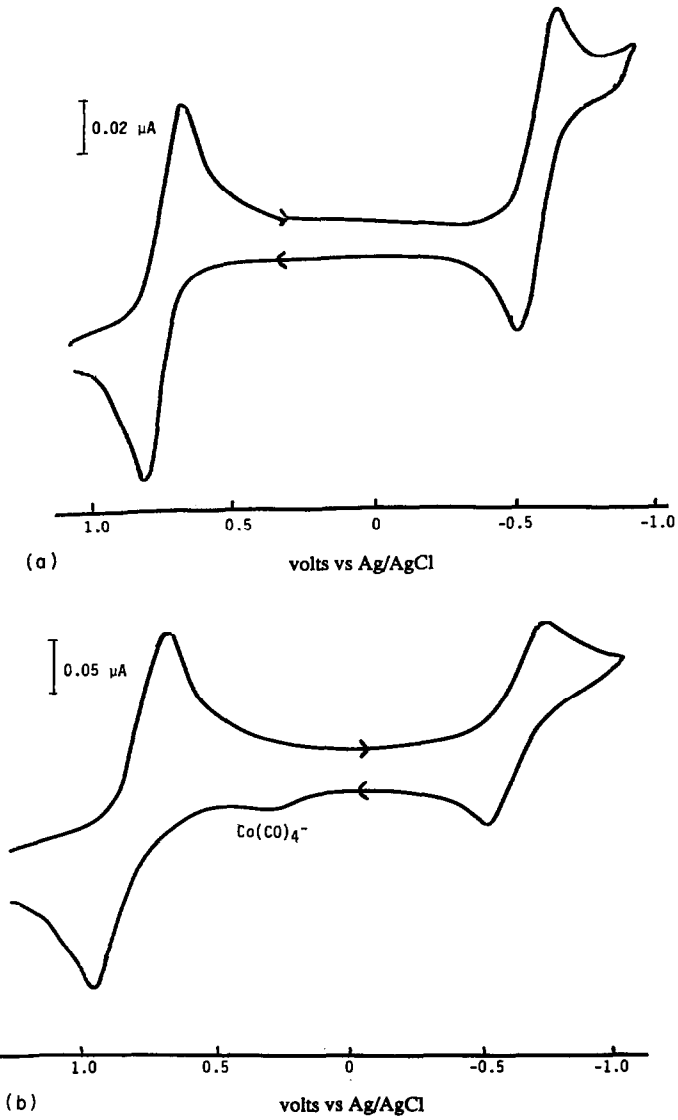

Fig. 2. Cyclic voltammogram in CH_2Cl_2 under Ar (295 K) at Pt. (a) **1a**: 50 mV s^{-1}; (b) **1b**: 200 mV s^{-1}.

$Fc'[Si(Me)_2CCo_3(CO)_9]_2^+$. A distinctive transition due to the ferricenium ion was observed at 610 nm (*cf.* 617 nm in FcH^+) [54], confirming that ferrocene is the redox centre. However, the ν(CO) profile was identical to that of $[FcSi(Me)_2CCo_3(CO)_9]^+$, underlining once more the mutual independence of the two cluster centres. These cations were stable in air for several hours as solids but rapidly reverted to the neutral complexes in solution.

Complex voltammetric responses were observed for the phosphine/phosphite derivatives but these are readily interpreted using the additivity relationships and $\vec{E}C\vec{E}$ mechanism noted above. **8**[1, 1] with one PPh_3 per CCo_3 showed identical electrochemistry to that of **4**[1], except that the reduction process required (de-

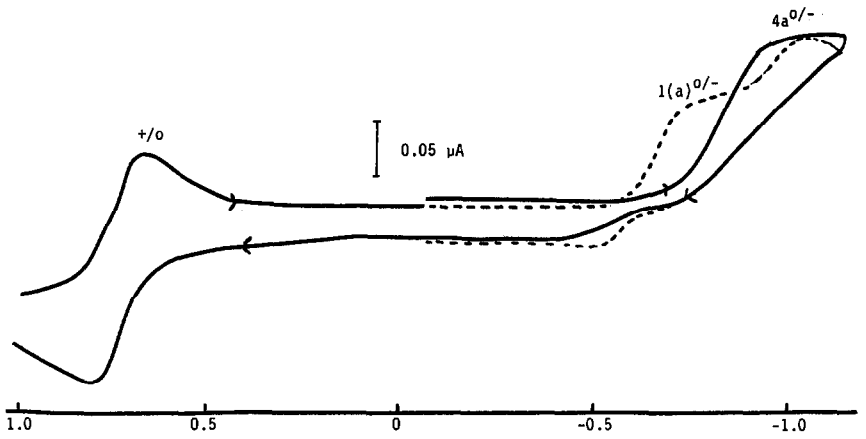

Fig. 3. Cyclic voltammogram of **4**[1] in CH_2Cl_2 under Ar (298 K) at Pt (200 mV s^{-1}); dotted line is the second scan.

pending on scan rate) up to 4e per molecule, with evidence for the formation of **2a** or **8**[0, 1] on repeat scans (Fig. 5).

Unsymmetrical substitution typified by **8**[0, 1] provides polarographic and voltammetric data which are essentially a superposition of responses from each individual redox centre (Fig. 6). Thus the chemically reversible one-electron transfer at -0.58 V is assigned to reduction of the $Me_2SiCCo_3(CO)_9$ moiety and that at -0.8 V to one-electron reduction of $Si(Me)_2CCo_3(CO)_8PPh_3$ followed by an $\vec{E}C\vec{E}$ process. The potentials for these reduction steps are virtually identical to

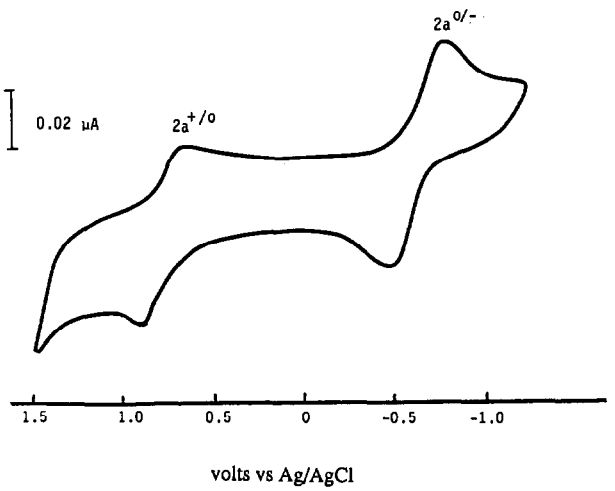

Fig. 4. Cyclic voltammogram of **2a** in CH_2Cl_2 under Ar (298 K) at Pt (100 mV s^{-1}); initial potential 0.0 V.

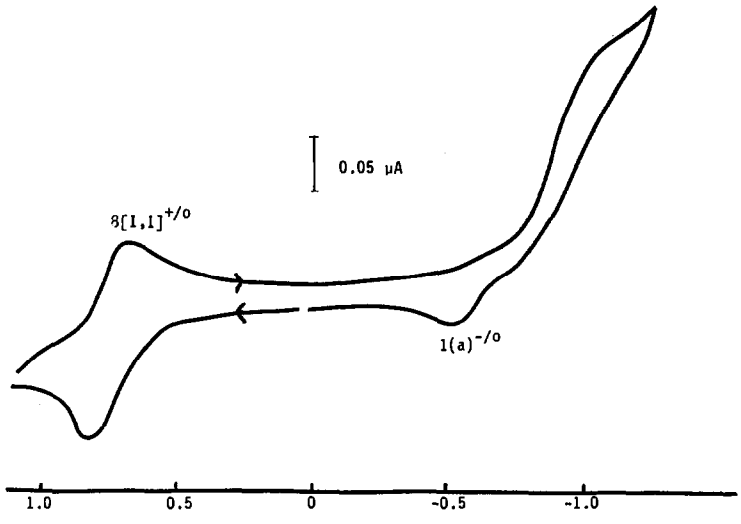

Fig. 5. Cyclic voltammogram of **8**[1, 1] in CH_2Cl_2 under Ar (298 K) at Pt (200 mV s^{-1}); initial potential 0.0 V.

those of **1a** and **4**[1] respectively, while the $E^{+/0}$ potential for the oxidation of the ferrocene moiety is the mean of the values for **1a** and **4**[1].

Interesting oxidation behaviour was observed for the bis-substituted Lewis base derivative **6**[2]. As $AgPF_6$ was added a new species was produced with an A_{t-sym}

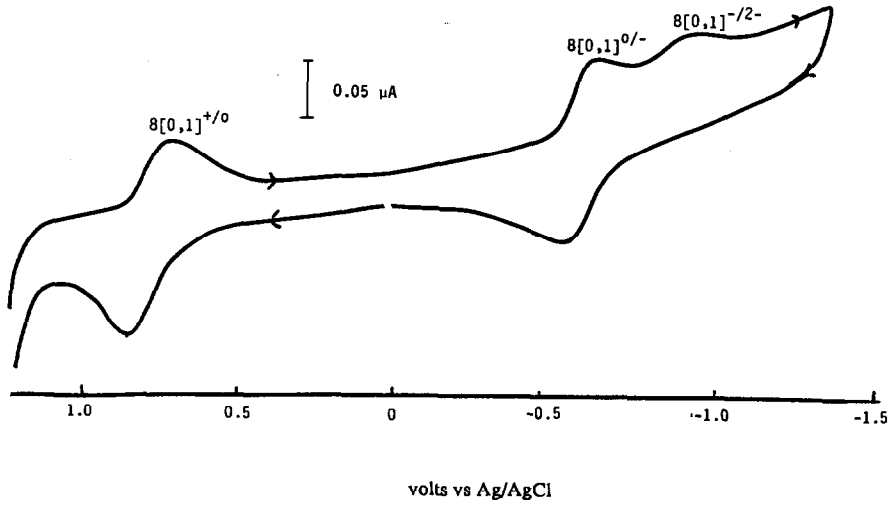

Fig. 6. Cyclic voltammogram of **8**[0, 1] in CH_2Cl_2 under Ar (298 K) at Pt (200 mV s^{-1}); initial potential 0.0 V.

ν(CO) band at 2111 cm^{-1}, 10 cm^{-1} higher than that for the neutral species. Furthermore, the ν(CO) profile was different to that of the neutral species and no ferrocenium transition was observed in the electronic spectrum. The shift in energy of the A_{t-sym} mode supports the premise that the cluster rather than the ferrocene cluster centre is oxidised despite oxidation of the ferrocene centre to give **6**[2]$^+$ being thermodynamically preferred at an electrode surface. Since there was no indication of the monocation in the ν(CO) spectra during the progressive addition of $AgPF_6$, we assume that a kinetically driven disproportionation reaction possibly under the influence of a silver complex, leads to the rapid production of **6**[2]$^{2+}$, the oxidised cluster centre being more stable than the mono-cationic derivative.

Conclusion

It is clear from this study that interpolation of silicon functionality between the ferrocene and tricobaltcarbon redox centres destroys the electronic communication established when the cluster is directly linked *via* carbon–carbon bonds to the ferrocene moiety. Lack of interaction between cluster redox centres has previously been observed in situations where the Co_3C units are linked via a bridging phosphine ligand such as dppe [22]. It may be that directional conducting materials containing the Co_3C unit will need carbon–carbon linkages. This restriction may simply arise because of the absence of suitable orbitals for overlap with the a_1 orbital of the cluster but the existence of significant steric interactions (presumably non-bonded interactions between the equatorial CO groups of the cluster and the ferrocene moiety) which influenced the reactivity of these molecules, was a surprise. Steric factors could make orbital overlap less efficient.

The volatility of the ferrocenylsilyl clusters and their propensity to disintegrate at relatively low temperatures make them ideal species for CVD work. Finally, the functionality on the silicon could allow the synthesis of macrocyclic cavities incorporating the Co_3C cluster.

Acknowledgments

We thank the University of Otago for a studentship (J.B.), and Dr Ward T. Robinson, University of Canterbury, for diffractometer facilities.

References and notes

1 F.L. Carter (Ed.), Molecular Electronic Devices, Marcel Dekker, New York, 1984.
2 A.J. Aviram, J. Am. Chem. Soc., 110 (1988) 5687.
3 A.L. Kaloyeros, J.W. Corbett, P.J. Toscano and R.B. Rizk, Mater. Res. Soc. Simp. Proc., 192 (1990) 601.
4 S.B. Colbran, B.H. Robinson and J. Simpson, Organometallics, 2 (1983) 943.
5 S.B. Colbran, B.H. Robinson and J. Simpson, Organometallics, 2 (1983) 952.
6 S.B. Colbran, B.H. Robinson and J. Simpson, Organometallics, 3 (1984) 1344.
7 For leading references see M. Bousseau, L. Valade, J.-P. Legros, P. Cassous, M. Garbauskas and L.V. Interrante, J. Am. Chem. Soc., 108 (1986) 1908.
8 M.B. Robin and P. Day, Adv. Inorg. Chem. Radiochem., 10 (1967) 247.
9 S.B. Colbran, L.R. Hanton, B.H. Robinson, W.T. Robinson and J. Simpson, J. Organomet. Chem., 330 (1987) 415.
10 G.H. Worth, PhD Thesis, University of Otago, 1986; G.H. Worth, B.H. Robinson and J. Simpson, Organometallics, in preparation.

11 K.M. Mackay and B.K. Nicholson, in G. Wilkinson, F.G.A. Stone and E.W. Abel (Eds.), Comprehensive Organometallic Chemistry, Vol. 6, Pergamon, Oxford, 1982, Chap. 43, p. 1043.
12 D. Seyferth, C.N. Rudie and M.O. Nestle, J. Organomet. Chem., 178 (1979) 227.
13 B.M. McGillen, BSc Hons. Thesis, University of Otago, 1984.
14 A.N. Nesmeyanov, E.G. Perevalova, R.N. Golovnya and O.A. Nesmeyanova, Dokl. Akad. Nauk SSSR, 97 (1954) 459.
15 D. Seyferth, H.P. Hofman, R. Burton and J.F. Helling, Inorg. Chem., 1 (1962) 227.
16 M.D. Rausch and D.J. Ciappenelli, J. Organomet. Chem., 10 (1967) 127.
17 R.A. Miller, Diss. Abstr., 17 (1957) 2847.
18 H. Gilman and F.K. Cartledge, J. Organomet. Chem., 2 (1964) 447.
19 A.J. Downward, B.H. Robinson and J. Simpson, Organometallics, 5 (1986) 1122.
20 T.A. Blinka, B.J. Helmer and R. West, Adv. Organomet. Chem., 23 (1984) 193.
21 P.N. Lindsay, B.M. Peake, B.H. Robinson, J. Simpson, U. Honrath and H. Vahrenkamp, Organometallics, 3 (1984) 413.
22 B.M. Peake, B.H. Robinson, J. Simpson and D.J. Watson, Inorg. Chem., 16 (1977) 405.
23 A.J. Downward, B.H. Robinson and J. Simpson, Organometallics, 5 (1986) 1132.
24 N.S. Nemetkin, T.I. Cherneysheva and L.V. Barbare, Zh. Obsch. Khim., 34 (1964) 2258.
25 J.Y. Corey, D. Gust and K. Mislow, J. Organomet. Chem., 101 (1975) C7.
26 The numbering scheme adopted for the phosphine and phosphite derivatives in this paper designates an identifying number to the complex with the number of phosphorus donor substituents following, in brackets. For the dicluster species, the two bracketed numbers identify the number of non-carbonyl substituents on each of the cluster centres.
27 International Tables for X-ray Crystallography, Vol. 1, Kynoch Press, Birmingham, 1966.
28 The data processing program HILGOUT is based on the programs DRED (J.F. Blount) and PICKOUT (R.J. Doedens).
29 G.M. Sheldrick, SHELX-76, program for crystal structure determination, University of Cambridge, 1976.
30 International tables for X-ray crystallography, Vol. 4, Kynoch Press, Birmingham, 1974.
31 ABSORB, a major modification of AGNOST (L. Templeton and D. Templeton).
32 J. Borgdorff, PhD Thesis, University of Otago, 1986; J. Borgdorff, B.H. Robinson and J. Simpson, J. Organomet. Chem., in preparation.
33 T.W. Matheson, B.H. Robinson and W.S. Tham, J. Chem. Soc. A, (1971) 1457.
34 C.J. Cardin, W. Crawford, W.E. Watts and B.J. Hattway, J. Chem. Soc., Dalton Trans., (1979) 970.
35 R.L. DeKock, K.S. Wong and T.P. Fehlner, Inorg. Chem., 21 (1982) 3203; G.L. Geoffroy and R.A. Epstein, Inorg. Chem., 16 (1977) 2795.
36 R.K. Harris, J.D. Kennedy, W. McFarlane, in R.K. Harris and B.E. Mann (Eds.), NMR and the Periodic Table, Academic Press, London, 1978.
37 R.H. Cragg and R.D. Lane, J. Organomet. Chem., 277 (1984) 199.
38 F.H. Kohler, W.A. Geike and N. Hertkorn, J. Organomet. Chem., 334 (1987) 359.
39 D. Seyferth, Adv. Organomet. Chem., 14 (1976) 97.
40 B.R. Penfold and B.H. Robinson, Accounts Chem. Res., 6 (1973) 73.
41 S.F. Xiang, A.A. Bakke, H.W. Chen, C.J. Eyermann, J.L. Hoskins, T.H. Lee, D. Seyferth, H.P. Withers and W.L. Jolly, Organometallics, 1 (1982) 699.
42 C.M. Arewgoda, B.H. Robinson and J. Simpson, J. Am. Chem. Soc., 105 (1983) 1893.
43 B.H. Robinson and J. Simpson, in M. Chanon, M. Juillard, J.C. Poite (Eds.), Paramagnetic Organometallic Species in Activation/Selectivity, Catalysis, Vol. 257, NATO ASI Series, Kluwer, Dordrecht, 1989, p. 357.
44 A.J. Downard, B.H. Robinson and J. Simpson, Organometallics, 5 (1986) 1140.
45 P.A. Dawson, B.H. Robinson and J. Simpson, J. Chem. Soc., Dalton Trans., (1979) 1762.
46 A.J. Deeming, in G. Wilkinson, F.G.A Stone and E.W. Abel (Eds.), Comprehensive Organometallic Chemistry, Vol. 4, Pergamon, Oxford, 1982, Chap. 31.3, p. 1043.
47 K. Hirotsu, T. Higuchi and A. Shimado, Bull. Chem. Soc. Jpn., 41 (1968) 1557.
48 M.R. Churchill and J.J. Wormald, Inorg. Chem., 8 (1969) 716.
49 P. Seiler and J.D. Dunitz, Acta Crystallogr., Sect. B, 35 (1979) 1068, 2020.
50 W.F. Paton, E.R. Corey, J.Y. Corey, M.D. Glick and K. Mislow, Acta Crystallogr., Sect. B, 33 (1977) 268.
51 A.M. Bond, B.M. Peake, B.H. Robinson, J. Simpson and D.J. Watson, Inorg. Chem., 16 (1977) 410.

52 B.M. Peake, P.H. Rieger, B.H. Robinson and J. Simpson, Inorg. Chem., 18 (1979) 1000.
53 B.H. Robinson and J. Simpson, in preparation.
54 G. Wilkinson, J. Am. Chem. Soc., 74 (1952) 6146.
55 A.M. Bond, P.A. Dawson, B.M. Peake, P.H. Rieger, B.H. Robinson and J. Simpson, Inorg. Chem., 18 (1979) 1413.
56 J.B. Flanagan, S. Margel, A.J. Bard and F.C. Anson, J. Am. Chem. Soc., 100 (1978) 4248.